EXHIBIT II

[CANCER RESEARCH 64, 6537–6541, September 15, 2004]

Microregional Effects of Gemcitabine in HCT-116 Xenografts

Lynsey A. Huxham, Alastair H. Kyle, Jennifer H. E. Baker, Lani K. Nykilchuk, and Andrew I. Minchinton

Department of Medical Biophysics, British Columbia Cancer Research Centre, Vancouver, British Columbia, Canada

ABSTRACT

To examine the tumor microregional effects after gemcitabine administration to mice, we mapped the location of proliferating and hypoxic cells relative to vasculature in human colon cancer xenografts. The S-phase marker bromodeoxyuridine was used as a surrogate of drug effect and administered 2 hours before tumor excision, whereas vessel position and perfusion were assessed via staining for CD31 and intravenous injection of carbocyanine, respectively. Hypoxia was detected using pimonidazole. Images of the four markers were overlaid to reveal the spatial relationship between proliferation, vasculature, and hypoxia and to examine the microregional effects. Within 1 day after administration of 240 mg/kg of gemcitabine, proliferation throughout the tumor was completely inhibited. Over time, a recmergence of dividing cells occurred in relation to the distance from vasculature. Microregional analysis revealed that cells located distal to vasculature commenced cycling sooner than cells located proximal to vasculature. A similar trcnd was seen after multiple doses of gemcitabine (40 mg/kg on days 1, 4, 7, and 10). The possibility that the effect of gemcitabine could be attributed to changes in oxygenation was discounted after examining the vessel perfusion and patterns of hypoxia. The effect of gemcitabine was examined in multilayered cell culture, and at doses <30 μmol/L, a gradient in proliferation between the exposed and unexposed sides was observed. We show a differential effect on cell proliferation in relation to vasculature and conclude that cells distal to blood vessels are less affected by gemcitabine probably because of limited penetration.

INTRODUCTION

Inefficient delivery of drug from the blood to the cells comprising the extravascular compartment of solid tumors could result in cells distant from blood vessels receiving subtherapeutic exposures (1). As a result, some cells could survive, continue to proliferate, or become drug resistant, permitting tumor regrowth. Barriers to penetration in tumors include drug metabolism, binding to extracellular components, and large intervascular distances (2, 3). The effectiveness of the pyrimidine analog gemcitabine could depend, in part, on the extent of penetration into the extravascular compartment of the tumor. We recently have shown, using SiHa tumor xenografts, that the tumor penetration of bromodeoxyuridine (BrdUrd), a bromine analog of the nucleoside uridine, is dose dependent (4).

Gemcitabine (2,2 difluorodeoxycytidine) is a synthetic, fluorinated analog of cytidine and structurally related to cytarabine (ara-C) but unlike cytarabine is used clinically to manage solid tumors (5–7). The transport of gemcitabine into cells occurs via a family of nucleoside transporters (NTs), and studies have shown that tumors are resistant to gemcitabine if these transporters are not expressed (8). Blocking thymidylate synthase also increases the number of equilibrative-sensitive NTs expressed on the cell membrane, which can lead to increased gemcitabine sensitivity (9). The activity of transported drugs, such as gemcitabine, could be affected if the level of NT expression is altered as a function of distance from vasculature. Once inside the cell, gemcitabine is phosphorylated by deoxycytidine kinase and further converted to the diphosphate and triphosphate derivatives (6). Gemcitabine diphosphate interacts with RNase reductase, depleting the deoxyribonucleotide stores, and the triphosphate form incorporates into DNA and RNA and blocks DNA polymerase processing (10–12).

In vitro and *in vivo* studies have shown a substantial suppression of DNA synthesis after gemcitabine administration, but neither microregional effects relative to vasculature nor the kinetics of such an effect have been examined (13–15). Here we use DNA synthesis, via BrdUrd incorporation, as a marker of cell proliferation at different times after doses of gemcitabine from 20 to 360 mg/kg. Experiments administering 240 mg/kg showed that following an initial suppression of proliferation, the cells far from vasculature, on the border of necrosis, begin to reenter S phase 2 to 3 days later, and levels of BrdUrd labeling reached control levels far from vasculature 4 days after treatment. Multiple doses of gemcitabine (four doses at 40 mg/kg) were given 3 days apart and showed similar results, with cells distal to vasculature dividing 2 days after the final dose. Global variations in hypoxia and vascular perfusion did not occur, indicating tumor oxygenation was not affected.

To assess the influence of drug penetration and to address the problem of cells far from vasculature being quiescent and less intrinsically sensitive to gemcitabine, tissue penetration experiments were carried out using multilayered cell cultures (MCCs), which model the extravascular compartment of solid tumors (16–18). MCCs consist of discs of tumor tissue, typically ~200 μm thick, grown from cells seeded on a permeable membrane (16, 18). They are similar to multicellular spheroids (19) in that they exhibit a gradient in proliferation, but because MCCs grow as discs, this gradient forms as a mirror image from either side toward the middle. By exposing MCCs to gemcitabine from only one side, drug delivery to tissue can be examined independently of other factors.

MATERIALS AND METHODS

Cells. HCT-116 human colorectal carcinoma cells were purchased from American Type Culture Collection (Manassas, VA). Cells were maintained *in vitro* at 37.5°C with 5% CO_2/5% O_2 in MEM (Life Technologies, Rockville, MD) supplemented with 10% fetal bovine serum (Life Technologies). Cells were passaged every 3 to 5 days on reaching confluence.

Mice and Tumors. Female nonobese diabetic/severe combined immunodeficient (NOD/SCID) mice were bred and maintained in our institutional animal facility in accordance with the Canadian Council on Animal Care guidelines. The Animal Care Committee of the University of British Columbia approved the experiments described in this article. Mice were allowed free access to standard laboratory rodent food and water. HCT-116 cells (50 μL of 1.6×10^8 cells/mL) were implanted subcutaneously into the sacral region of the mice. The mice used were between 8 to 20 weeks of age and ranged in weight from 20 to 27 g. The weight of the excised tumors was 60 ± 23 mg (mean ± SD).

Treatment. Mice were treated when their tumor volume reached 100 mm^3 as measured using calipers and the formula $V = \pi/6(l \times h \times w)$. Gemcitabine was administered intraperitoneally at doses of 20, 40, 80, 160, and 360 mg/kg 24 hours before tumor excision, at 240 mg/kg and the tumors excised 1, 2, 3, 4, and 6 days later, or 40 mg/kg on days 1, 4, 7, and 10 and the tumors excised on days 9, 12, 14, 16, and 18. All of the mice were administered BrdUrd (Sigma Chemical, St. Louis, MO) 2 hours before tumor excision. BrdUrd was administered intraperitoneally as a 30-mg/mL solution in saline at 1500 mg/kg. Pimonidazole (Hypoxyprobe-1 kit; Chemicon International Inc., Temecula,

Received 3/19/04; revised 6/24/04; accepted 7/13/04.

Grant support: National Cancer Institute of Canada with funds from the Canadian Cancer Society. A. H. Kyle is a Michael Smith Foundation for Health Research and Canadian Institutes of Health Research scholar.

The costs of publication of this article were defrayed in part by the payment of page charges. This article must therefore be hereby marked *advertisement* in accordance with 18 U.S.C. Section 1734 solely to indicate this fact.

Requests for reprints: Andrew I. Minchinton, British Columbia Cancer Research Centre, 601 West 10th Avenue, Vancouver, British Columbia, V5Z 1L3, Canada. E-mail: aim@bccrc.ca

CA) was administered intraperitoneally to some mice 2 hours before tumor excision at 60 mg/kg. As a marker of blood vessel perfusion, all of the mice were intravenously administered ~75 μL of 0.6 mg/mL carbocyanine (Molecular Probes, Eugene, OR), dissolved in 75% DMSO, 5 minutes before sacrifice. After excision, tumors were cooled to ~20°C on an aluminum block, covered in embedding medium (Tissue-TEK OCT; Sakura Finetek, Torrance, CA), and stored at −80°C until sectioning.

Multilayered Cell Culture. Tissue culture inserts (CM, 12 mm; pore size, 0.4 μm; Millipore, Billerica, MA) were coated with 150 μL collagen (rat tail type I; Sigma), dissolved in 0.01 mol/L HCl, diluted 1:4 with 60% EtOH to 0.75 mg/mL, and allowed to dry overnight. HCT-116 (0.75×10^6 cells in 0.5 mL growth media) then was added to the inserts and incubated for 15 hours to allow the cells to attach. The cultures then were incubated for 2 days in a custom-built growth vessel to form multilayered cultures ~150 μm thick. Each growth vessel contained a frame that held the inserts completely immersed in 130 mL of stirred media (700 rpm and 25-mm stir bar) under continual gassing (5% CO_2, balance air) at 37°C. The MCCs were grown in batches of eight cultures of which six were treated with drug and two were kept as untreated controls.

MCC Penetration Assay. MCCs were exposed to gemcitabine from one side using a polyacrylate jig designed such that the bottom of each insert was clamped against a flat block with a layer of Parafilm (American National Can, Chicago, IL) sandwiched between to ensure a complete seal. Each MCC was incubated with 7.5 mL stirred media kept under controlled gassing and temperature. A silicone O-ring was used to seal the gap between the MCC and the orifice in the reservoir. Once placed in the jig, MCCs were allowed to equilibrate for 45 minutes, and drug then was added to the growth medium at concentrations of 3, 10, 30, and 100 μmol/L. After 1-hour drug exposure, the reservoirs were rinsed twice with fresh media. MCCs then were incubated for a second hour before removal from the jig to allow initial drug washout from the top side only. MCCs then were removed, rinsed in fresh media three times for 15 seconds, and placed in a growth vessel containing two untreated control MCCs. Media were replaced at 1 and 4 hours following return to the growth vessel to reduce residual drug levels. Incubation with control MCCs allowed us to rule out the possibility that drug washout into the media from the exposed sides of the MCCs was affecting results. MCCs were left for 1 or 3 days from the time of drug exposure to allow manifestation of drug effect. Following this, 100 μmol/L BrdUrd (Sigma Chemical) were added to the media, and cultures were incubated for 4 hours to label S-phase cells. MCCs then were removed, frozen in Tissue-TEK OCT medium, and stored at −80°C until sectioning.

CD31 and Pimonidazole Immunohistochemistry. Tumor cryosections (10 μm thick) were cut with a Cryostar HM560 (Microm International GmbH, Walldorf, Germany), air dried for 24 hours, then fixed in a 1:1 mixture of acetone-methanol for 10 minutes at room temperature, and blocked with 3% H_2O_2. Vasculature was stained using a platelet/endothelial cell adhesion molecule/CD31 antibody (1:100 dilution; BD PharMingen, San Diego, CA), and bound pimonidazole was detected using Hypoxyprobe-1 Mab1 (1:50 Hypoxyprobe-1 kit; Chemicon International Inc.). An Alexa 546 goat antirat secondary (1:50 dilution; Molecular Probes) was used to detect CD31, and an Alexa 488 goat antimouse secondary (1:100 dilution; Molecular Probes) was used to detect pimonidazole. Primary antibodies were added together, and the secondary antibodies were added separately, all in 2% goat serum. Slides then were mounted with PBS and imaged (see Image Acquisition).

BrdUrd Immunohistochemistry. After the slides were imaged for vasculature and pimonidazole (if used), they were rinsed in PBS, placed in distilled water for 10 minutes, and then treated with 2 mol/L HCl at room temperature for 1 hour, followed by neutralization for 5 minutes in 0.1 mol/L sodium borate. Slides then were washed in distilled water and transferred to a PBS bath. Subsequent steps were each followed by a 5-minute wash in PBS. Incorporated BrdUrd was detected using a monoclonal mouse anti-BrdUrd (1:200 dilution, clone BU33; Sigma), followed by an antimouse peroxidase conjugate antibody (1:100 dilution; Sigma) and a metal enhanced DAB substrate (1:10 dilution; Pierce, Rockford, IL). Slides then were counterstained with hematoxylin, dehydrated, and mounted using Permount (Fisher Scientific, Hampton, NH) before imaging. For the MCCs, cryosections (10 μm) were air dried for 24 hours and then fixed in a 1:1 mixture of acetone-methanol for 10 minutes at room temperature. Slides were immediately transferred to distilled water for 10 minutes and stained following the aforementioned procedure.

Image Acquisition. The imaging system consisted of a fluorescence microscope (III RS; Zeiss, Oberkochen, Germany), a cooled monochrome charge-coupled device video camera (model 4922; Cohu, San Diego, CA), frame grabber (Scion, Frederick, MD), a custom-built motorized x-y stage, and customized NIH Image software (http://rsb.info.nih.gov/nih-image/) running on a G4 Macintosh computer (Apple, Cupertino, CA). The motorized stage allowed for tiling of adjacent microscope fields of view. Using this system, images of entire tumor sections were captured, typically 25 to 50 mm^2 in size, at a resolution of 1 pixel/μm^2. Images of carbocyanine fluorescence within the sections were obtained before CD31 immunostaining using a 450- to 480-nm excitation filter and a 525-nm long pass emission filter. Once immunostained for CD31, slides were imaged under PBS using a 510- to 555-nm excitation filter and a 575- to 640-nm emission filter. Slides stained for pimonidazole were imaged under PBS using the same filter set as for carbocyanine. The slides then were immunostained for BrdUrd, and bright field images of BrdUrd positive staining were obtained. Once the images were acquired, the layers were stacked; the CD31 and carbocyanine layers were thresholded; and a composite color image was produced with the grayscale BrdUrd/tissue layer.

Image Analysis. Using the NIH Image software application and user-supplied algorithms, images of carbocyanine fluorescence, CD31 fluorescence, and BrdUrd/tissue staining from each tumor section were overlaid, and areas of necrosis and staining artifacts were removed. For CD31 and BrdUrd images, by selecting all of the pixels that were 2.5 SD above background levels, positive regions were identified. CD31-positive regions that were <5 μm^2 in size were considered artifacts and removed from the analysis. Measuring the distance from each point in the tissue to the nearest CD31-positive pixel and noting whether it was BrdUrd positive or negative then determined the relation between proliferation and distance to the nearest blood vessel. The data were tabulated to determine the fraction of BrdUrd-positive pixels of the total number of pixels found at each distance to a blood vessel. The fraction of BrdUrd-positive tissue then was expressed as a fraction of the controls, for which the averaged control level was 1, by dividing the treated values at each distance by the value for the average of all of the controls at that distance. The fraction of perfused vessels was determined by comparing CD31 and carbocyanine labeling of vasculature. Raw images for the two stains were first thresholded to identify positive staining 5 SD above background. On the CD31 images, positively stained objects then were counted and classified as perfused if they were colabeled by carbocyanine (minimum 10% of pixels in each object). Objects <5 μm^2 in size were ignored.

RESULTS

HCT-116 tumor-bearing mice were treated with gemcitabine, and the total fraction of BrdUrd labeling was assessed at various times after administration. This tumor type was chosen because it exhibits a corded structure, with necrosis occurring ~150 μm from blood vessels, which facilitates assessment of microregional effects in relation to vasculature. In this tumor, complete cessation of proliferation was evident 1 day after administration of gemcitabine at doses ranging from 20 to 360 mg/kg, and quantitative analysis showed that overall BrdUrd labeling was reduced to <3% of the control levels irrespective of dose. We examined the kinetics of this suppression in mice administered 240 mg/kg gemcitabine. The initial suppression of proliferation was followed by a gradual resumption in proliferation occurring over 6 days to 66% of the control levels (Fig. 1*A*). Multiple doses of gemcitabine, 40 mg/kg administered on days 1, 4, 7, and 10, resulted in a similar initial decrease in proliferating cells, followed by a return of labeling to 64% of the control levels 8 days after the end of dosing (Fig. 1*B*).

The microregional effects of gemcitabine were analyzed by examining composite tumor images and measuring the distance of BrdUrd-labeled cells from the vasculature. Examples of small portions from composite images and the corresponding analysis of tumors excised on various days after 240 mg/kg of gemcitabine are shown in Fig. 2; the perivascular staining of carbocyanine is shown as light blue; the endothelial cells labeled for CD31 are dark blue; and cells incorpo-

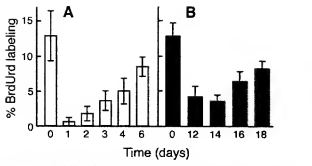

Fig. 1. Gemcitabine induces a complete cessation of proliferation after 1 day. *A*, BrdUrd labeling following a single dose of gemcitabine (240 mg/kg) on day 0. *B*, BrdUrd labeling on days 12, 14, 16, and 18 after four doses of gemcitabine (40 mg/kg on days 1, 4, 7, and 10). Untreated tumors are marked as day 0. Graphs show the means of tumors ($n = 3$ to 5) ± SD.

rating BrdUrd are grayscale. Consistent with our previous studies in SiHa xenografts, the analysis of untreated tumors showed division throughout the tumor, with a labeling fraction decreasing from ~20% in cells proximal to vasculature to ~10% in cells on the border of necrosis distal to vasculature (Fig. 2*A*; ref. 4). One day after treatment with gemcitabine, proliferation halts throughout the tumor, and after 4 days cell proliferation returns far from vasculature (Fig. 2*C*). Quantitative analysis of complete tumor images confirms the fraction of BrdUrd-labeled cells distal to vasculature returns to control levels at a faster rate than those cells proximal to the vasculature (Fig. 2*B*). The level of BrdUrd labeling 2 days after treatment is <20% of control levels for cells within 75 μm of a blood vessel, and cells distal are ~50% of the control level. However, by days 4 to 6, the levels of proliferation far from vasculature have reached control levels, whereas those near vasculature are ~50% of control levels.

Administering multiple doses of gemcitabine at 40 mg/kg shows a similar trend to a single dose by analysis and visually, whereby cells far from vasculature are dividing 2 days after ending treatment, and over time proliferation slowly returns near vasculature (Fig. 3). Twelve days from the first dose of gemcitabine, the cells far from vasculature remain at control levels of division, whereas cells near the vasculature have <25% labeling. Finally, 18 days after treatment began (8 days after the end of treatment), the tumors are returning to control levels of labeling, and those cells 75 to 150 μm from vasculature label at control levels, whereas those cells near vasculature are at 50% of the control levels. Interestingly, tumors excised on day 9, before the final dose of gemcitabine, are similar to those excised on day 12, and the analysis for both shows 25% of the labeling of controls near vasculature; however, cells far from vasculature label at control levels, indicating cells are cycling distal to vasculature before the next dose of gemcitabine is administered.

To determine the effect of gemcitabine on tumor oxygenation, pimonidazole was administered to a subset of mice. Composite images showed no apparent change in hypoxia between untreated and treated tumors, whereby hypoxia was detected on the edges of necrosis and in patches within the tumor distant from vasculature. The controls show no division on the edge of the tumor cords or in the pimonidazole-labeled region; however, 2 to 3 days after treatment, the cells divide at the edge of necrosis and can be seen in the regions labeled with pimonidazole (Fig. 4). Vascular perfusion also did not change between treated (73 to 82 ± 7.3% perfusion) and untreated tumors (75 ± 10% perfusion) nor did we observe large areas where entire cords become hypoxic.

MCCs were used to examine the role of tissue penetration on the efficacy of gemcitabine indcpendently of the effect of the gradient in proliferation that occurs with depth into tissue. MCCs, 175 μm thick, were exposed to gemcitabine for 1 hour from one side over a range of concentrations and then incubated for 1 or 3 days to allow for manifestation of drug effect. Fig. 5 shows cryosections of MCCs 1 and 3 days after gemcitabine exposure, which occurred from the upper side of the sections. Untreated MCCs exhibit a high level of proliferation on either side, with reduced proliferation toward the central area. One day after treatment of MCCs (Fig. 5*A*), the effect of gemcitabine on proliferation is confined to the exposed sides of the cultures at the low concentrations, and only at ≥30 μmol/L is its effect seen throughout the tissue. MCCs incubated for 3 days following 1-hour gemcitabine exposures are shown in Fig. 5*B*. In this case, the untreated MCC was removed only 1 day after drug exposure for comparison with the data in Fig. 5*A*. Three days after treatment of MCCs (Fig. 5*B*), the gradient of effect is consistent with the results

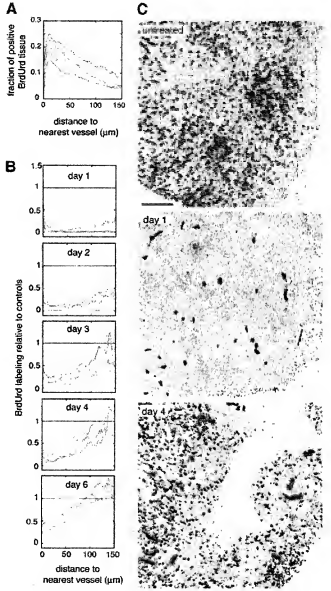

Fig. 2. The resumption of proliferation depends on proximity to vasculature. *A*, the fraction of BrdUrd-positive tissue with distance to vasculature for untreated tumors. The corresponding image of an untreated tumor is shown in *C*, untreated. *B*, the analysis of BrdUrd labeling relative to the controls 1, 2, 3, 4, and 6 days after treatment. Each line for the analysis graphs represents data from an individual tumor. *C*, examples of composite tumor images for an untreated tumor and for days 1 and 4 after treatment with 240 mg/kg of gemcitabine. The composite images are shown as a visual example and represent only 10% of the actual tumor cryosection used for individual analysis. *Dark blue*, vasculature; *light blue*, perfusion; *black*, dividing cells; *bar*, 150 μm.

seen 1 day after treatment; however, the regions that initially showed complete cessation of proliferation now exhibit a scattered return of S-phase cells. For unknown reasons, cells on the top and bottom layers of the MCCs showed proliferation 1 day after exposure; however, 3 days after exposure this effect was not observed.

DISCUSSION

Assessment of drug penetration into tissue is hindered by the inability to directly visualize drugs in tissue. In this study we have used BrdUrd incorporation as a marker for cell proliferation and therefore a surrogate for the effect of antiproliferative drugs on tissue. By quantitatively analyzing the location of affected cells relative to the position of the nearest blood vessel, we can evaluate the extent of drug effect.

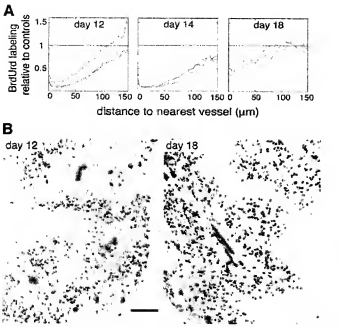

Fig. 3. Cell proliferation is evident distal to vasculature after multiple doses of gemcitabine. *A*, the analysis of BrdUrd labeling relative to controls *versus* the distance to the nearest vessel on days 12, 14, and 18 days after the first dose of gemcitabine (40 mg/kg on days 1, 4, 7, and 10). Each line for the analysis grapha represents data from an individual tumor. *B*, portions of composite tumor images on days 12 and 18 after the first day of treatment. The composite images shown represent only 10% of the actual tumor cryosection used for analysis. *Dark blue*, vasculature; *light blue*, perfusion; *black*, dividing cells; *bar*, 150 μm.

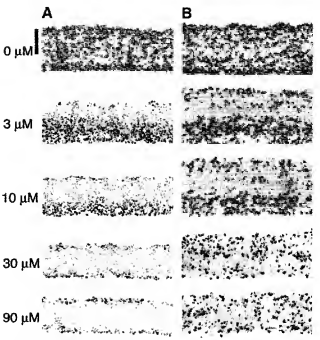

Fig. 5. Effect of gemcitabine in MCCs 1 and 3 days after a 1-hour exposure to the top side of the cultures. Panels show BrdUrd labeling (*black*) in cells 1 (*A*) and 3 days (*B*) after exposure to 0, 3, 10, 30, and 90 μmol/L gemcitabine for 1 hour; *bar*, 150 μm.

Tumors from mice treated with 240 mg/kg gemcitabine, near the weekly maximum tolerated dose in mice (20), show a dramatic cessation of proliferation throughout the tumor, but during subsequent days cell proliferation resumed initially in areas distal to vasculature. If cells within the tumor were equally affected by gemcitabine, one would expect resumption in proliferation to occur first in cells close to blood vessels rich in nutrients and oxygen. However, we found the opposite occurs, suggesting all of the cells are exposed to gemcitabine, but its effects are greatest on cells proximal to blood vessels. We hypothesize that a gradient of drug concentration could result in cells proximal to the

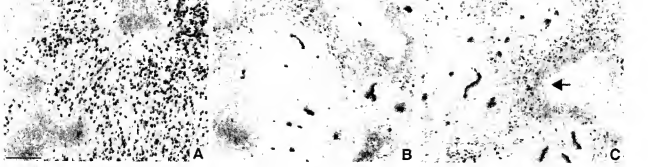

Fig. 4. Proliferation occurs in regions labeled with pimonidazole. Composite images of tumors treated with 240 mg/kg of gemcitabine and stained for hypoxia. *A–C*, untreated, 2 day, and 3 days after treatment, respectively. Arrows indicate proliferating regions on the edge of necrosis. The composite images shown represent only 10% of the actual tumor cryosection used for analysis. *Dark blue*, vasculature; *light blue*, perfusion; *black*, dividing cells; *green*, hypoxia; *bar*, 150 μm.

vasculature being affected more than cells residing distally. This is consistent with observations *in vitro* showing cells exposed to gemcitabine for 1 hour at concentrations of ≤100 nmol/L cause a G_1 block, the length of which is dose specific (15), and multilayered cell culture experiments suggesting at concentrations <30 μmol/L there is a gradient in effect related to drug exposure. The radial geometry of a tumor creates a greater barrier to penetration than the planar diffusion through MCCs.

Interestingly, cells located on the border of necrosis, which appear quiescent in untreated tumors, began to proliferate after gemcitabine treatment. These quiescent cells may not be affected by gemcitabine because of inadequate exposure to drug, their noncycling status, or insensitivity caused by down-regulation of NTs on the cell membrane. One hypothesis for the return to cycle of the quiescent cells is that an increased oxygen supply, resulting from the effects of gemcitabine on cells closer to blood vessels, may have allowed these cells to start proliferating. To test this, we examined the pattern of hypoxia in tumors by administering pimonidazole. No change in hypoxia was observed, discounting the possibility that cells return to division because of reoxygenation. Furthermore, because hypoxia is mainly seen bordering necrosis in treated and untreated tumors and because vascular perfusion was not changed, the effects of gemcitabine were not mediated by changes in vessel perfusion.

Although the quiescent cells may be intrinsically less sensitive to gemcitabine and therefore able to divide after drug exposure, they constitute only the last two or three layers of cells. Control levels of proliferation are reached at 75 to 150 μm from vessels 4 to 6 days after gemcitabine administration, indicating most cells at these distances, despite being sensitive at the time of exposure, were able to resume cycling. When multiple doses of gemcitabine were administered, cells were dividing far from vasculature on day 9, before the last dose, showing these distal cells were cycling and likely sensitive to gemcitabine when the final dose was administered; however, cells still return to cycle 2 days after the last dose.

Our studies using a range of doses from 20 to 360 mg/kg of gemcitabine to test the concentration dependence on proliferation show a dose-independent virtually complete cessation of tumor cell proliferation 24 hours after gemcitabine administration. This is not unexpected because the toxicity of gemcitabine, unlike other pyrimidine analogs, is not confined to cells in S phase at the time of drug administration because of the long intracellular retention time (12, 15, 21). The kinetics of the proliferation resumption have not been explored at each dose, but flow cytometry experiments, using BrdUrd to detect S-phase cells, indicate DNA synthesis begins to recover in SA-NH tumors administered 10 mg/kg gemcitabine after 12 hours, whereas it takes 24 to 36 hours for DNA synthesis to recover after 400 mg/kg of gemcitabine (14). Therefore, beyond 24 hours, the resumption of proliferation throughout the HCT-116 tumor could be faster for low doses of drug and take days for higher doses as is seen with 240 mg/kg of gemcitabine.

The current clinical protocol for gemcitabine administration commonly indicates a 30-minute intravenous infusion of 33 to 40 mg/kg (1000 to 1200 mg/m^2) on days 1, 8, and 15 for every 28 days (20, 21). The peak plasma concentration for humans administered this protocol is 15 to 20 μmol/L, and for mice administered a single dose of 240 mg/kg, it is >100 μmol/L with a plasma half-life of 15 minutes (20, 21). MCCs show a concentration-dependent wave of proliferation inhibition 1 day after a 1-hour drug exposure for which ≥30 μmol/L gemcitabine is required to halt division through 150 μm of tissue. Three days later, these cells return to cycle throughout the MCCs, indicating that even a 90-μmol/L exposure for 1 hour does not prevent the cells from returning to division. *In vivo* cells near the vasculature may be exposed to concentrations >100 μmol/L and not return to cycle until >6 days later, or undergo apoptosis. However, the cells far from vasculature may receive lower concentrations of drug, which allows them to return to cycling 2 or 3 days later. In the MCC experiments, the discrete wave of proliferation inhibition observed is likely to be the result of the defined steady-state exposure and the planar geometry of the culture. Tumor distribution is the result of a more complex drug-exposure profile dictated by the *in vivo* pharmacokinetics and a more complex three-dimensional geometry.

Mice administered multiple doses of gemcitabine 3 days apart show cells cycling far from vasculature 2 or 3 days after the final dose, similar to that seen after a single dose. Therefore, multiple doses do not appear to enhance drug delivery because the resumption of proliferation follows similar kinetics as a single dose of gemcitabine. A study by Cividalli *et al.* (22) shows the tumor growth delay in CH3/TIF mammary adenocarcinomas is 18 days when gemcitabine is administered on days 1, 4, 7, and 10 and was reduced to 12.2 days if 5 days were left between doses, suggesting multiple doses given too far apart will allow cells to begin proliferating before another dose is given and therefore lead to a smaller tumor growth delay.

In conclusion, gemcitabine administration results in a complete cessation of proliferation in all of the cells throughout the tumor; however, over time cells distal from vasculature resume cycling, and eventually the tumor approaches control levels of proliferation. This suggests a differential effect of drug on cells as a function of their location to the tumor vasculature.

REFERENCES

1. Tannock IF, Lee CM, Tunggal JK, Cowan DS, Egorin MJ. Limited penetration of anticancer drugs through tumor tissue: a potential cause of resistance of solid tumors to chemotherapy. Clin Cancer Res 2002;8:878–84.
2. Jain RK. Vascular and interstitial barriers to delivery of therapeutic agents in tumors. Cancer Metastasis Rev 1990;9:253–66.
3. Jain RK. The next frontier of molecular medicine: delivery of therapeutics. Nat Med 1998;4:655–7.
4. Kyle AH, Huxham LA, Baker JHE, Burston HE, Minchinton AI. Tumor distribution of bromodeoxyuridine-labeled cells is strongly dose dependent. Cancer Res 2003;63:5707–11.
5. Hertel LW, Kroin JS, Misner JE. Synthesis of 2-deoxy-2',2'-difluoro-D-ribose and 2-deoxy-2',2'-difluoro-D-ribofuranosyl nucleosides. J Org Chem 1988;53:2406–9.
6. Heinemann V, Hertel LW, Grindey GB, Plunkett W. Comparison of the cellular pharmacokinetics and toxicity of 2',2'-difluorodeoxyuridine and 1-β-D-arabinofuranosylcytosine. Cancer Res 1988;48:4024–31.
7. Hertel LW, Boder GB, Kroin JS, et al. Evaluation of the antitumor activity of gemcitabine (2',2'-difluoro-2'-deoxycytidine). Cancer Res 1990;50:4417–22.
8. Mackey JR, Mani RS, Selner M, et al. Functional nucleoside transporters are required for gemcitabine influx and manifestation of toxicity in cancer cell lines. Cancer Res 1998;58:4349–57.
9. Rauscher DR, Firby PS, Hedley DW, Moore MJ. Equilibrative-sensitive nucleoside transporter and its role in gemcitabine sensitivity. Cancer Res 2000;60:6075–9.
10. Plunkett W, Huang P, Xu YZ, et al. Gemcitabine: metabolism, mechanisms of action, and self-potentiation. Semin Oncol 1995;22(Suppl 11):3–10.
11. Heinemann V, Xu YZ, Chubb S, et al. Inhibition of ribonucleotide reduction in CCRF-CEM cells by 2',2'-difluorodeoxycytidine. Mol Pharmacol 1990;38:567–72.
12. Plunkett W, Huang P, Searcy CE, Gandhi V. Gemcitabine: preclinical pharmacology and mechanisms of action. Semin Oncol 1996;23(Suppl 10):3–15.
13. Wexler EJ, Gravallese EM, Czerniak PM, et al. Tumor biology: use of tiled images in conjunction with measurements of cellular proliferation and death in response to drug treatments. Clin Cancer Res 2000;6:3361–70.
14. Millar L, Fuji T, Hunter N, et al. Enhancement of tumor radioresponse in vivo by gemcitabine. Cancer Res 1999;59:107–14.
15. Cappella P, Tomasoni D, Faretta M, et al. Cell cycle effects of gemcitabine. Int J Cancer 2001;93:401–8.
16. Cowan DSM, Hicks KO, Wilson WR. Multicellular membranes as an in vitro model for extravascular diffusion in tumours. Br J Cancer 1996;74:S28–31.
17. Kyle AH, Chan CT, Minchinton AI. Characterisation of three dimensional tissue cultures using electrical impedance spectroscopy. Biophys J 1999;76.
18. Minchinton AI, Wendt KR, Clow KA, Fryer KH. Multilayers of cells growing on a permeable support: an in vitro tumour model. Acta Oncol 1997;36:13–6.
19. Sutherland RM. Cell and environment interactions in tumor microregions: the multicell spheroid model. Science 1988;240:177–84.
20. Veerman G, Ruiz van Haperen VW, Vermorken JB, et al. Antitumor activity of prolonged as compared with bolus administration of 2',2'-difluorodeoxycytidine in vivo against murine colon tumors. Cancer Chemother Pharmacol 1996;38:335–42.
21. Chabner BA, Ryan DP, Paz-Ares L, Garcia-Carbonero R, Calabresi P. Antineoplastic agents. In: Hardman JG, Limbird LE, Goodman Gilman A, editors. Goodman and Gilman's the pharmacological basis of therapeutics. New York: McGraw-Hill; 2001. p. 1410–1.
22. Cividalli A, Mauro F, Livdi E, et al. Schedule dependent toxicity and efficacy of combined gemcitabine/paclitaxel treatment in mouse adenocarcinoma. J Cancer Res Clin Oncol 2000;126:461–7.